Extended winter Pacific North America oscillation as a precursor of the Indian summer monsoon rainfall

Y. Peings, Hervé Douville, Pascal Terray

Extended winter Pacific North America oscillation as a precursor of the Indian summer monsoon rainfall

Y. Peings, H. Douville

CNRM/GAME, Météo-France/CNRS, Toulouse, France

P.Terray

LOCEAN, Institut Pierre Simon Laplace (IPSL), Paris, France

Corresponding author address:

Yannick Peings
CNRM/GMGEC/UDC, 42 avenue Gaspard Coriolis
31057 Toulouse Cedex 01, France

Email: yannick.peings@cnrm.meteo.fr

Abstract

In spite of considerable efforts, long-range forecasting of Indian summer monsoon rainfall (ISMR) is still a challenge for both statistical and dynamical tools. We highlight the winter-to-spring Pacific North America (PNA) oscillation as a predictor for the ISMR. A PNA-related index is proposed that is highly correlated with the following summer precipitation over India and is also a precursor of El Niño-Southern Oscillation (ENSO) events over recent decades. The PNA index compares well with other predictors used in operational statistical models for ISMR prediction. A multiple linear regression scheme is tested with a cross-validation hindcast approach and confirms the added value of our predictor, at least over the period 1958-2005. Nevertheless, the predictor shows less skill over the first half of the 20th century. Possible physical mechanisms of this teleconnection are also briefly discussed and could involve both a tropical Pacific sea surface temperature and Eurasian snow cover pathway.

Keywords

Statistical seasonal forecasting, Indian summer monsoon, Pacific North America oscillation, El Niño-Southern Oscillation, Eurasian snow cover.

1. Introduction

Forecasting Indian summer monsoon rainfall (ISMR) is of great importance for the livelihoods of more than one billion of people and for India's economy. Year-to-year fluctuations of the amount of precipitation received during the monsoon season (June to September) can cause severe droughts or floods which dramatically affect the agricultural sector and have an adverse impact on economies and societies in South Asia. The influence of El Niño-Southern Oscillation (ENSO) on Asian monsoon variability has been extensively documented by both observational and numerical studies and is now widely recognized by the climate community [Soman and Slingo, 1997]. An inverse relationship has been established between the East Equatorial Pacific sea surface temperature (SST) and the ISMR, with a positive (negative) phase of ENSO associated with a deficient (heavy) monsoon rainfall over India. However, this relationship exhibits strong multi-decadal variability and has diminished since the 1980's [Kripalani and Kulkarni, 1997; Krishna Kumar et al., 1999]. Moreover, ENSO predictability shows a significant spring barrier so that the Pacific SST cannot be used as an efficient predictor of the Indian summer monsoon [Webster et al, 1992].

Though many efforts have been conducted over recent decades for developing both statistical and dynamical tools, the long-range forecasting of ISMR remains a challenge for the climate community [Gadgil et al., 2005]. Statistical predictions are based on more-or-less established relationships between ISMR and various climate parameters considered as potential predictors, like regional anomalies in SST or atmospheric circulation observed a few months, seasons or years before the summer monsoon. Dynamical predictions rely on coupled or forced general circulation models (GCMs) and therefore have a more physical basis, but do not necessarily outperform statistical schemes given the difficulty of state-of-the-art GCMs in simulating the salient features of the monsoon climate [Wang et al., 2005]. In view of these

51 results, the Indian Meteorological Department (IMD)'s operational seasonal forecasting
52 system is still based on statistical models using a relatively large number of predictors with a
53 two-stage strategy: a first forecast is issued in mid-April and a second one by the end of June.
54 Recently, more robust multiple linear regressions were developed with a lower number of
55 predictors after the failure of the operational forecasts in 2002 and 2004 [Rajeevan et al,
56 2006].

57 The present study is aimed at suggesting a new predictor for improving the ISMR
58 hindcasts (and hopefully forecasts) issued by the IMD. This predictor is related to a well-
59 known atmospheric circulation pattern, the Pacific North America (PNA) oscillation [Wallace
60 and Gutzler, 1981]. The loading pattern of the PNA is characterized by alternating centres of
61 anomalous pressure that arc north-eastward through the North Pacific Ocean, through Canada,
62 and then curve south-eastward into North America. Its link with ENSO has been extensively
63 studied but the role of tropical pacific SST in triggering or amplifying internal modes of
64 variability such as the PNA is still a matter of debate [Trenberth et al., 1998; Straus et al.,
65 2002]. The PNA influence on regional temperature and precipitation is well established, but
66 few studies have focused on its possible remote impacts. Using both reanalyses and coupled
67 ocean-atmosphere simulations, Yu et al. (2008) suggest that ENSO controls only ¼ of the
68 PNA variability, which in turn has apparently a limited influence on tropical diabatic heating
69 in boreal winter. Here we demonstrate that a PNA index averaged over winter and spring
70 shows a significant statistical relationship with the subsequent Indian summer monsoon and
71 can be used as an efficient predictor of IMSR in a simple multiple linear regression scheme.
72

73 2. Data and methods

74 To represent the ISMR, we use the June to September (JJAS) seasonal mean All India
75 Rainfall (AIR) index available over the 1871-2005 period, an area-weighted average from 29

Indian Rainfall subdivisions [Parthasarathy et al., 1995]. GPCC (Global Precipitation Climatology Centre) precipitation reanalyses for the 1901-2007 period were downloaded at http://gpcc.dwd.de. Sea level pressure (SLP) and 500hPa geopotential height (Z500) monthly fields are derived from the European Centre for Medium-Range Weather Forecasts (ECMWF) reanalyses (1958-2001) and operational analyses (2002-2007), a dataset which will be named ERA50 hereafter. Global SSTs are derived from the Hadley Centre climatology (HadSST) available over the 1870-2006 period. We also use the Hadley Centre SLP climatology (HadSLP) available over the 1850-2003 period (http://hadobs.metoffice.com/index.html). The equatorial Pacific upper ocean heat content (mean temperature between 0 and 300 meters depth) was derived from SODA reanalyses [Carton et al., 2000]. To remove global warming effect, all time series have been detrended using a simple linear fit before computing seasonal anomalies.

3. Results

3.1. PNA-monsoon relationship

A monthly PNA index is first constructed according to the Wallace and Gutzler definition [Wallace and Gutzler, 1981] based on the Z500 distribution and is averaged from December to May (DJFMAM). This index is strongly correlated with the ISMR index over the 1958-2005 period (correlation coefficient $R=0.47$, $p<0.001$). Figure 1a shows the regression of the summer precipitation and of 850 hPa wind over the DJFMAM PNA index. The positive relationship with the monsoon rainfall is clearly visible, a cyclonic anomaly over India and an increase of the moist south-westerly flow over the Arabian sea driving more precipitable water towards the Indian subcontinent.

To have a wider perspective on the PNA-monsoon relationship, a pseudo-PNA index was also computed from the HadSLP sea level pressure climatology (1850-2003). Figure 1b shows the correlation pattern of SLP reanalyses with the original PNA index over the 1958-2007 period. The strongest correlation is found over the two centres located over the North Pacific ocean (see markers on Figure 1b), so that it was decided to keep only this dipole pattern in the calculation of our pseudo-PNA index (hereafter called the "North Pacific Dipole index"):

$$NPDI = SLP^{*}(20°N\text{-}160°W) - SLP^{*}(45°N,165°W)$$

where SLP are standardized mean sea level pressure values. As suggested in Figure 2a, the DJFMAM NPDI computed with ERA50 is highly correlated with ISMR for the period 1958-2005 ($R=0.56$ and $p=0.0001$). The NPDI is therefore a better predictor of the Indian monsoon than the original PNA index of Wallace and Gutzler (1981). These correlations suggest that a positive DJFMAM anomaly of the PNA oscillation during winter and spring is followed by strong monsoon rainfall over India in the following summer, and *vice versa*. The individual correlations between ISMR and the two parts of the dipole are 0.43 and -0.41 with the subtropical and north Pacific centre of action respectively. Thus, they both play a role in the NPDI-ISMR correlation.

To assess the contribution of the NPDI compared to a canonical ENSO index, Figure 2b shows the lead-lag monthly correlations between ISMR and the monthly timeseries of NPDI and Niño-3.4 index (i.e. the average JJAS SST anomalies in the 120°W-170°W/ 5°S-5°N domain). The monthly time series have been smoothed using a 5-month sliding window in order to increase the signal to noise ratio. The maximum NPDI correlation (black curve) with summer monsoon rainfall appears in March, when the Niño-3.4 correlation (red curve) shows a rapid decline. The NPDI is thus less sensitive to the spring predictability barrier than ENSO and therefore represents an interesting precursor of the monsoon. The Niño-3.4 index

126 correlation with the DJFMAM NPDI (blue curve) shows that the ENSO variability leads the
127 NPDI by several months, but also suggests that the NPDI is itself a potential precursor of
128 ENSO. This feature is more than an artefact due to the quasi periodicity of ENSO, since the
129 NPDI- Niño-3.4 index correlation is stronger than the Niño-3.4 SST autocorrelation.

130 Figure 2c shows the sliding correlations between the NPDI computed with the
131 HadSLP2 data, the ISMR index and the Niño-3.4 index. The NPDI-ISMR relationship (solid
132 black line) is strong and stable during recent decades, but was not significant in the first half
133 of the 20th century and in the late 19th century. The ENSO-ISMR relationship (solid red line)
134 is more stable, but shows an apparent weakening over recent decades [Torrence and Webster,
135 1999]. This weakening has been attributed to several reasons such as global warming
136 [Krishna Kumar et al., 1999], stochastic noise [Gershunov et al., 2001], or more recently
137 Atlantic SST variability [Kucharski et al, 2008]. The strong PNA-monsoon relationship is
138 observed since the 1960s, a period characterized by a significant lead-lag PNA-ENSO
139 relationship (solid blue line). It suggests that the strong NPDI-ISMR correlation during recent
140 decades could result from the apparent influence of the PNA oscillation on the ENSO
141 development. We speculate that a possible mechanism could be the persistence of the PNA in
142 a particular phase during winter months involves circulation and SST anomalies in the North
143 and equatorial Pacific. An anticyclonic (cyclonic) circulation, associated with a positive
144 (negative) NPDI, is associated with a strengthening (weakening) of the easterly winds near
145 the equator. This modulation of the easterly winds can affect the intraseasonal occurrence of
146 westerly wind bursts which are known to play a role in the triggering of ENSO events
147 [McPhaden et al. 1998; Belamari et al., 2003].

148 These results suggest that the PNA-monsoon predictive relationship is embedded in a
149 broader ENSO-PNA-monsoon system. However, the partial correlation between the
150 DJFMAM NPDI and ISMR, with the JJAS Niño-3.4 SST influence removed by linear

151 regression, remains significant ($R=0.44$, $p<0.01$). This residual correlation suggests that,
152 besides tropical Pacific SST, there is another pathway between the winter/spring PNA and the
153 following summer monsoon variability.

154 A recent study of the Eurasian snow-Indian monsoon relationship has emphasized that
155 the eastern Eurasian snow depth in spring was positively correlated with the subsequent
156 ISMR between 1966 and 1995 [Peings and Douville, 2009]. The PNA oscillation is one of the
157 extratropical circulation modes which modulates the snow depth variability over Eurasia
158 [Popova, 2007]. Indeed, the NPDI exhibits a strong correlation with the eastern Eurasian
159 snow depth over this period (close to 0.6). We hypothesize that the snow-monsoon
160 relationship might therefore be a consequence of the PNA influence on both spring snow
161 cover and subsequent Indian summer monsoon. Alternatively, it might also be evidence of
162 another PNA-monsoon pathway through an active role of the Eurasian snow cover. This topic
163 is beyond the scope of the present study and will need further investigation, including
164 sensitivity experiments with atmospheric GCMs.

165 To help understand the multi-decadal variability of the PNA-ISMR and ENSO-ISMR
166 relationships, we have computed the standard deviation of the NPDI over a 31-year sliding
167 window (dashed black line on Figure 2c). The strength of the NPDI correlation with ISMR
168 (and ENSO) is in phase with the epochal variations of the NPDI variance during the 20th
169 century. This result suggests that the NPDI influence vanishes when its year-to-year
170 variability is not strong enough.

171

172 3.2. Implications for the statistical prediction of ISMR

173

174 The next step is to assess if the NPDI can be useful in the context of statistical
175 forecasting, using a multiple linear regression model as in Rajeevan et al. (2006). The list of

their predictors used for the two-stage models (i.e. April and June forecasting) is given in Table 1, as well as their respective correlation coefficient (CC) with the ISMR index over the period 1958-2005. We have derived the same predictors from the datasets described in Section 2 and our results are therefore slightly different. Except for two first stage predictors, all correlations are significant at the 99% confidence level and the DJFMAM NPDI exhibits the strongest correlation with ISMR. Among the other ISMR predictors, correlations with NPDI are significant for Niño-3.4 SST anomaly tendency (J4, R=-0.47), equatorial south east Indian Ocean SST anomaly (A2/J2, R=0.44), and Equatorial Pacific upper ocean heat content (A6, R=-0.40). It suggests that NPDI has some connection with Indo-Pacific SST variability, which does not mean that it is not as well the expression of internal extratropical atmospheric dynamics. To discuss the added value of our new ISMR predictor, we have compared different multiple linear regression schemes using a leave-one out cross validation over the period 1958-2005. This method consists in comparing observed ISMR values with those calculated from the regression schemes based successively on all years except the forecast year. For each stage, this comparison has been made between all possible combinations from the pool of one to seven predictors shown in Table 1.

To assess the models's skill, we have used the correlation coefficient R between the 38 predicted and observed ISMR values, the Root-Mean-Square-Error (RMSE) and a generalized cross-validation (GCV) function computed as given below:

$$GCV = \frac{\sum (Y'-Y)^2 / n}{(1 - p/n)^2}$$ with Y' the model forecast, Y the observed value, n the number of years and p the number of predictors. GCV is nearly equal to the square of the RMSE with a correction for the number of predictors used in the model. Table 2 summarizes the two best models for each stage, with and without the NPDI as a predictor (A7 and J7).

For the second stage, the ISMR prediction is considerably improved with the correlation coefficient between observed and predicted values increased by 0.08, i.e. an

increase of more than 10% of explained variance with the addition of the NPDI in the list of potential predictors. For the first stage the improvement is less pronounced (about 7% increase of explained variance). Figure 3 shows the ISMR time series for 1958-2005 and the predicted values for the two forecasting stages. An interesting feature of the models integrating the NPDI predictor is a better ability to capture extreme values of monsoon rainfall, and in particular the droughts of 2002 and 2004 which were not predicted by operational statistical models.

4. Discussion and conclusions

This study highlights the lead correlation between a winter-to-spring PNA-related index and the following Indian summer monsoon rainfall during recent decades. Our index is computed several months before the monsoon onset and may therefore be useful for operational seasonal forecasting.

Understanding the physical mechanisms that control the interannual variability of the PNA-monsoon system remains a difficult challenge and will require further investigation. This relationship seems partly associated with the ENSO variability and with its influence on Indian monsoon. However, the NPDI-ISMR relationship remains significant after the removal of ENSO effects through simple linear regression, suggesting that the NPDI influence on the summer Indian monsoon has another pathway. In line with the results of Peings and Douville (2009), a contribution of the eastern Eurasian snow cover has been proposed and will be tested in a modelling study with the CNRM atmospheric GCM.

Finally, the implications of our new monsoon predictor for the statistical prediction of ISMR have been briefly explored. In keeping with the two stages of the IMD operational seasonal forecasting system, a multiple linear regression scheme has been tested, which is

226 based on a pool of seven potential predictors (including the NPDI). A simple cross-validation
227 approach has been applied over the period 1958-2005 for all possible models. The results
228 show that including the NPDI in the pool of predictors yields better skill, with an increase of
229 about 7% in the explained variance of ISMR for the first stage, and 10 % for the second
230 forecast stage. This increase has been obtained over a relatively long period (1958-2005) and
231 the new regression improves in particular the hindcast of the 2002 and 2004 deficient
232 monsoon seasons, which were poorly predicted by the operational IMD forecasting system.
233 Note however that a single model approach has been used to assess the relevance of our NPDI
234 predictor and that its potential contribution to a multi-model [Rajeevan et al., 2006; Sahai et
235 al., 2008] empirical forecasting system remains to be evaluated.

236 Moreover, the PNA-monsoon relationship is not stable over the entire 20th century.
237 The strengthening of the NPDI variability observed since the 1950's could be an explanation
238 for the increasing influence of the PNA oscillation on both Indian monsoon and ENSO, but
239 this needs further analysis.

240

241 **Acknowledgements:** We are thankful to Alexander Gershunov, Aurélien Ribes and
242 anonymous reviewers for their constructive comments and suggestions to improve the quality
243 of the paper.

244

245

246 References

247

248 Belamari, S., J.L. Redelsperger and M. Pontaud (2003), Dynamic role of a westerly wind
249 burst in triggering an equatorial Pacific warm event, *J. Clim.*, 16,1869–1890.

250

Carton, J. A., G. Chepurin, X. Cao, and B. Giese (2000), A simple ocean data assimilation analysis of the global upper ocean 1950 – 95—part I: Methodology, *J. Phys. Oceanogr*., 30, 294 – 309.

Gadgil, S., M. Rajeevan and R. Nanjundiah (2005), Monsoon prediction - why yet another failure? *Curr. Sci*., 84, 1713-1719.

Gershunov, A., N. Schneider and T. Barnett (2001), Low-frequency modulation of the ENSO-Indian monsoon rainfall relationship: signal or noise? *J. Clim.*, 14, 2486-2492.

Kripalani, R. H. and A. Kulkarni (1997), Climatic impact of El Niño/ La Niña on the Indian monsoon: A new perspective, *Weather*, 52, 39– 46.

Krishna Kumar K., B. Rajagopalan and M.A. Cane (1999), On the Weakening Relationship Between the Indian Monsoon and ENSO, *Science, 284*, 2156-2159.

Kucharski, F., A. Bracco, J.H. Yoo and F. Molteni (2008), Atlantic forced component of the Indian monsoon interannual variability, *Geophys. Res. Lett*., 35, L04706, doi:10.1029/2007GL033037.

McPhaden, M.J. et al. (1998), The Tropical Ocean-Global Atmosphere observing system: A decade of progress, *J. Geophys. Res.*, 103, 14, 169-240.

Parthasarathy B., A. Munot and D.R. Kothawale (1995), Monthly and seasonal rainfall series for All India homogeneous regions and meteorological subdivisions: 1871-1994, Contrib.

Indian Inst. Trop., *Meteorol. Res. Rep. RR-065*, 113, Indian Inst. of Trop. Meteorol., Pune, India, Aug.

Peings, Y. and H. Douville (2009), Influence of the Eurasian snow cover on the Indian summer monsoon variability in observed climatologies and CMIP3 simulations, *Clim. Dyn*., submitted.

Popova, V. (2007), Winter snow depth variability over northern Eurasia in relation to recent atmospheric circulation changes, *Int. J. Climatol*., 27, 1721-1733.

Rajeevan, M., D.S. Pai, R. Anil Kumar and B. Lal (2006), New statistical models for long-range forecasting of southwest monsoon rainfall over India, *Clim. Dyn.*, 28, 813-828.

Sahai, A.K., R. Chattopadhyay and B.N. Goswami (2008), A SST based large multi-model ensemble forecasting system for Indian summer monsoon rainfall, *Geophys. Res. Lett.*, 35, L19705, doi:10.1029/2008GL035461.

Soman, M. K. and J. Slingo (1997), Sensitivity of the Asian summer monsoon to aspects of SST anomalies in the tropical Pacific Ocean, *Q. J. R. Meteorol. Soc*., 123, 309– 336.

Straus, D. M. and J. Shukla (2002), Does ENSO force the PNA?, *J. Clim.*, 15, 2340–2358.

Torrence, C. and P. Webster (1999), Interdecadal changes in the ENSO-monsoon system. *J. Clim.*, 12, 2679-2690.

301 Trenberth, K.E. et al. (1998), Progress during TOGA in understanding and modeling global
302 teleconnections associated with tropical sea surface temperatures, *J. Geophys. Res.*, 103, 14,
303 291-324.
304
305 Wallace, J.M. and D.S. Gutzler (1981), Teleconnections in the geopotential height field
306 during the Northern Hemisphere winter*, Mon. Weather Rev.,* 109, 784–812.
307
308 Wang, B., Q. Ding, X. Fu, I.-S. Kang, K. Jin, J. Shukla and F. Doblas-Reyes (2005),
309 Fundamental challenge in simulation and prediction of summer monsoon rainfall, *Geophys.*
310 *Res. Lett*., 32, L15711, doi:10.1029/2005GL022734.
311
312 Webster, P.J. and S.Yang (1992), Monsoon and ENSO: Selectively interactive systems, *Q. J.*
313 *R. Meteorol. Soc, 118, 877-926.*
314
315 Yu B., Y.M. Tang, X.B. Zhang and A. Niitsoo (2008), An analysis on observed and simulated
316 PNA associated atmospheric diabatic heating. *Clim. Dyn*., doi:10.1007/s00382-008-0432-4.
317

a)

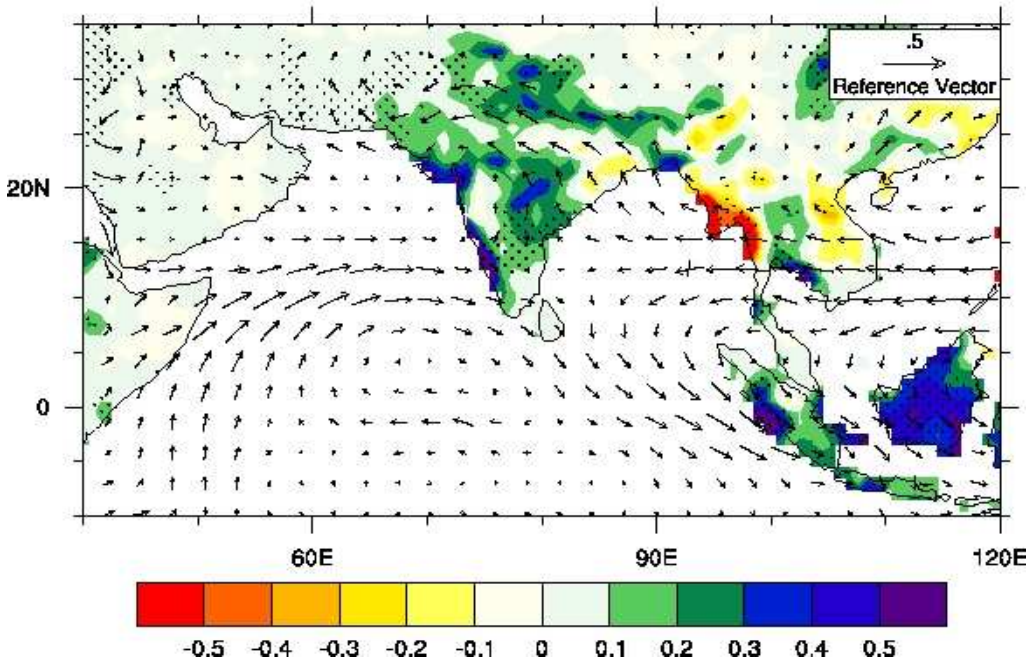

b)

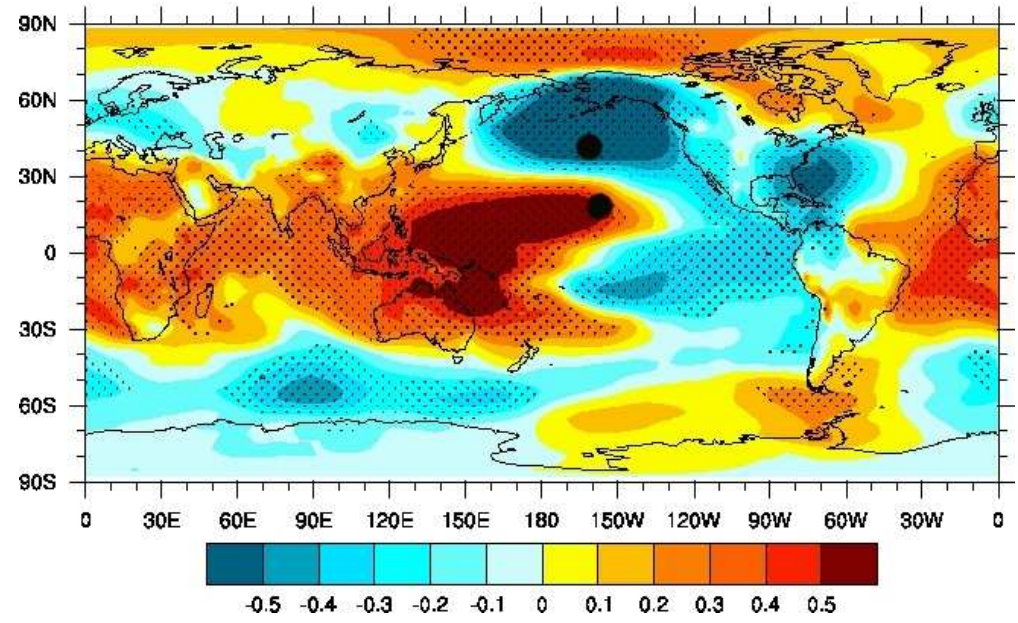

Figure 1. (a) Regression onto the DJFMAM PNA index of the JJAS GPCC precipitation (mm) and 850 hPa wind vector (m/s), over the period 1958-2007. (b) Correlation between the DJFMAM PNA index and the DJFMAM SLP, over the period 1958-2007. Black dots indicate the NPDI centres locations and stippled areas represent the 90% confidence level (for precipitation in a).

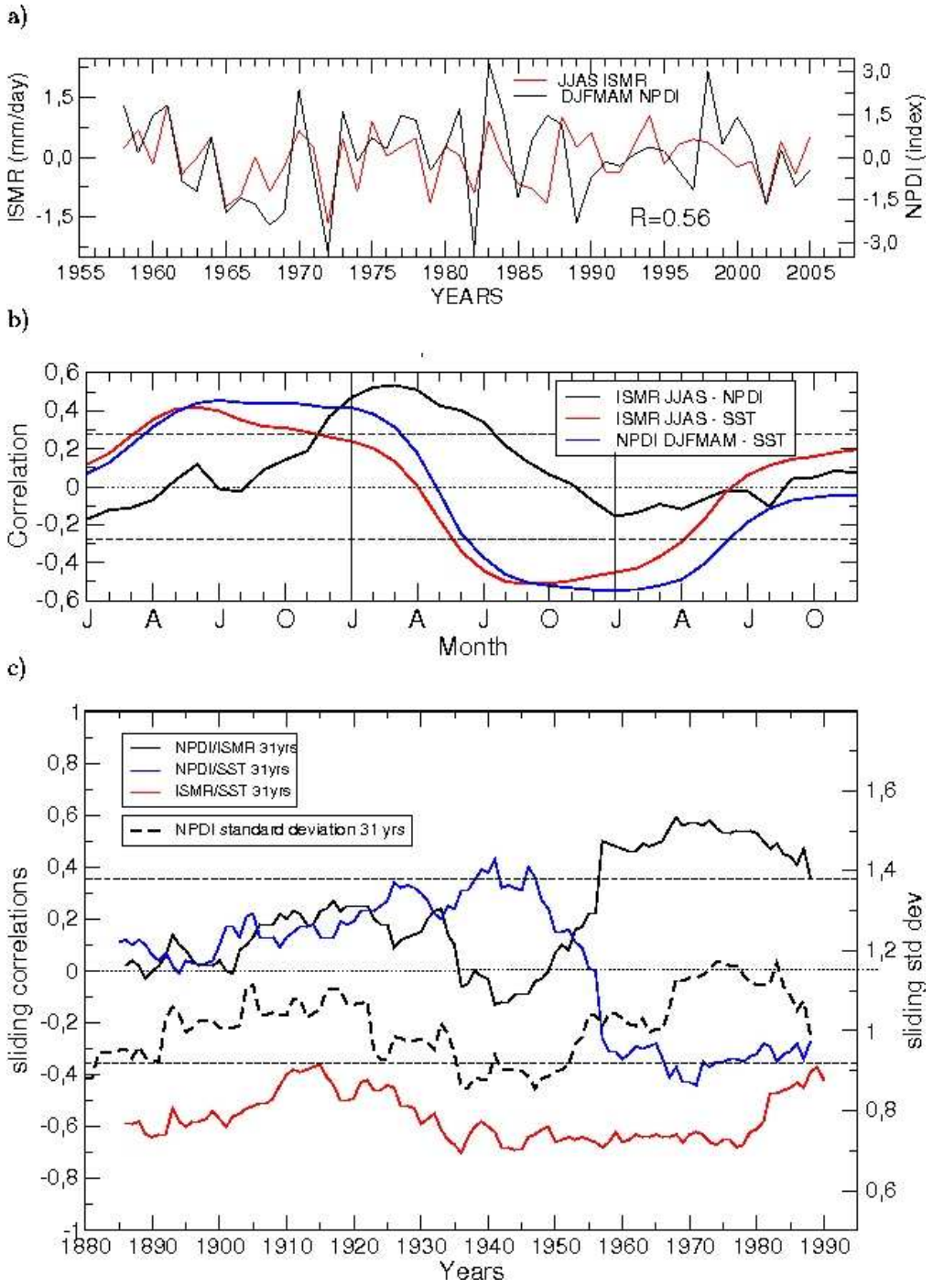

Figure 2. (a) Time series of the detrended DJFMAM NPDI and the ISMR index over the 1958-2005 period. (b) Lead/lag correlations over 1958-2005 between monthly NPDI and ISMR (black), monthly Niño-3.4 SST and ISMR (red), monthly Niño-3.4 SST and DJFMAM NPDI (blue). The monthly time-series are averaged over a 5 months sliding window. (c) 31-years sliding correlations between DJFMAM NPDI, ISMR and JJAS SST n34, and 31-years sliding standard deviation of DJFMAM NPDI during the 20th century. The dashed lines correspond to the 95% confidence level.

a)

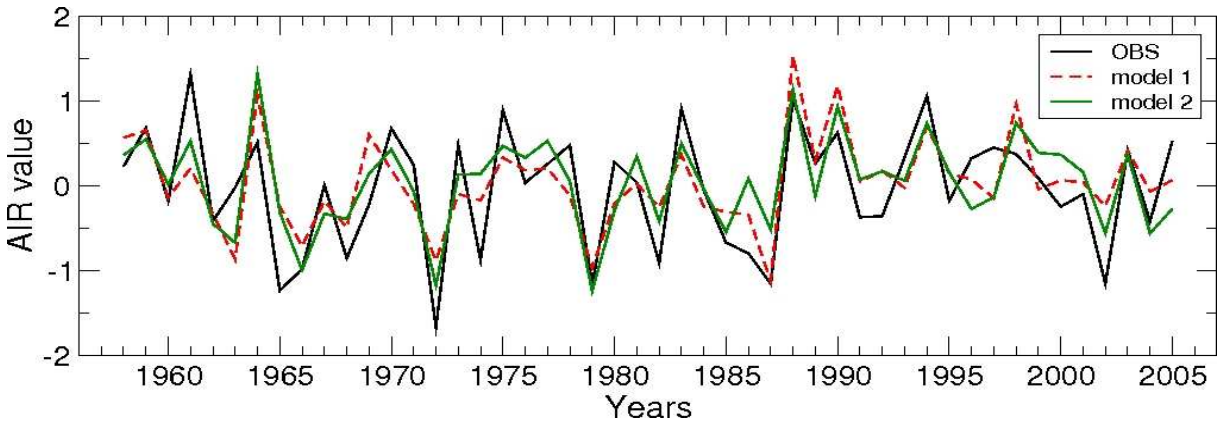

b)

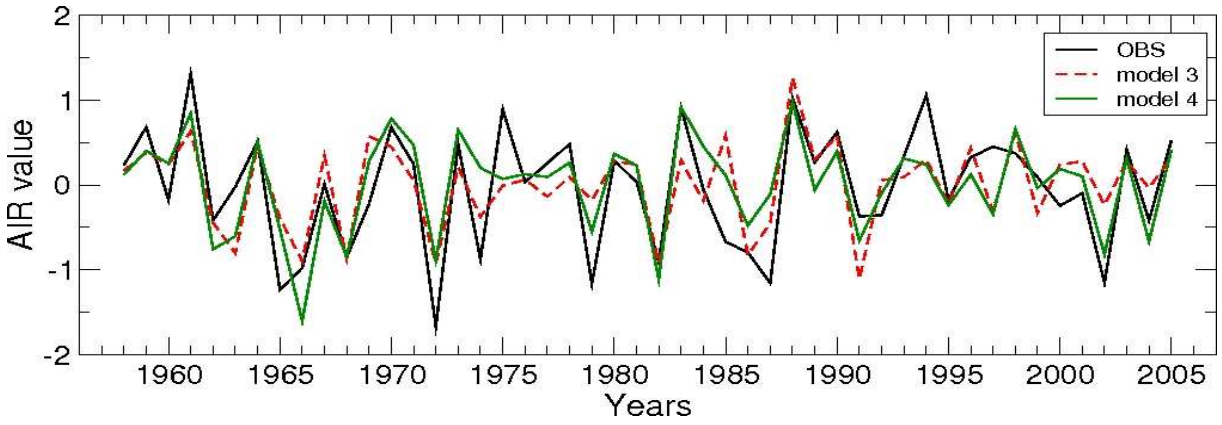

Figure 3. Time series of the JJAS ISMR index (solid black line) and of its predicted values (mm/day) for: (a) first forecasting stage, (b) second forecasting stage, over the period 1958-2005. Green (Red) curves represent the models with (without) NPDI as predictor, and black curves show observed values of ISMR.

Parameter	Period	Domain	CC with ISMR (1958-2005)
A1-J1 North Atlantic SST anomaly	December-January	20N-30N, 100W-80W	-0.38*
A2-J2 Equatorial SE Indian Ocean SST anomaly	February-March	20S-10S, 100E-120E	0.42*
A3-J3 East Asia surface pressure anomaly	February-March	35N-45N, 120E,130E	0.43*
A4 Europe surface temperature anomaly	January	35N-60N, 10W-30E	0.42*
A5 Northwest Europe surface pressure anomaly tendency	DJF(0)-SON(-1)	65N-75N, 20E-40E	-0.27
A6 Equatorial Pacific upper ocean heat content	February+March	4°S-4°N, 140°E-90°W	-0.16
J4 Niño-3.4 SST anomaly tendency	MAM-DJF	5S-5N, 170W-120W	-0.41*
J5 North Atlantic surface pressure anomaly	May	35N-45N, 30W-10W	-0.46**
J6 North Central Pacific zonal wind anomaly at 850 hPa	May	5N-15N, 180E-150W	-0.41*
A7 NPDI DJFM	December-March	See Definition	0.46**
J7 NPDI DJFMAM	December-May	See Definition	0.56**

* $p < 0.01$; ** $p < 0.001$

Table 1. Details of predictors used for the first stage forecast (predictors A) and for the second stage forecast (predictors J) of ISMR and comparison with the NPDI predictors.

Model	R	RMSE (mm/day)	GCV (mm/day)²
Stage 1 (mid of April)			
Model 1 : A1-A2-A3-A4-A5	0.70	0.49	0.30
Model 2 : A1-A3-A4-A5-A7	0.75	0.46	0.27
Stage 2 (end of June)			
Model 3 : J1-J2-J5-J6	0.68	0.50	0.30
Model 4 : J3-J5-J6-J7	0.76	0.45	0.24

Table 2. Comparison of the two better models of ISMR prediction over the period 1958-2005, with and without the NPDI (A7 and J7), for the two stage of forecasting. The results are obtained by multiple linear regression realized with a leave-one-out cross validation.